24-norursodeoxycholic acid reshapes immunometabolism in CD8$^+$ T cells and alleviates hepatic inflammation

Ci Zhu, Nicole Boucheron, André C. Müller, Peter Májek, Thierry Claudel, Emina Halilbasic, Hatoon Baazim, Alexander Lercher, Csilla Viczenczova, Daniela Hainberger, Teresa Preglej, Lisa Sandner, Marlis Alteneder, Alexandra F. Gülich, Matarr Khan, Patricia Hamminger, Jelena Remetic, Anna Ohradanova-Repic, Philipp Schatzlmaier, Clemens Donner, Claudia D. Fuchs, Tatjana Stojakovic, Hubert Scharnagl, Shinya Sakaguchi, Thomas Weichhart, Andreas Bergthaler, Hannes Stockinger, Wilfried Ellmeier, Michael Trauner

Table of contents

Supplementary materials and methods

Flow Cytometric Analysis

Single cell suspensions of spleen and liver of *in vivo* models were obtained through mechanical disruption through 70µm cell strainers. Intrahepatic T cells were enriched following gradient separation[1]. Total cell count was normalized to tissue weight. Murine peripheral blood was treated by Lyse/Fix buffer (BD) for 10min at 37 °C and cells permeabilized with Perm/Wash I buffer (BD) for 30min on ice. Staining with anti-pRPS6 Abs (Cell Signaling) was performed for 30min on ice together with antibodies listed in Table S1. For circulating immune cells assessment, blood was pipetted into Heparin containing tubes and treated with RBC lysis buffer (eBioscience). Samples were then treated with FcR-Block (Clone 93, eBioscience), and subsequently stained with the respective antibodies as indicated in each experiment. Tetramer staining (GP33/GP276/NP396-specific tetramers from NIH Tetramer Core Facility, US) was performed at 37°C for 15min prior to FcR-block treatment.

Murine $CD8^+$ T cells cultured for 48h with plate-bound anti-CD3/anti-CD28 Abs were stimulated under indicated conditions and fixed for 10min at 37°C with Cytofix (BD), permeabilized 20min on ice with methanol and stained with the indicated phospho-Abs for 30min in the dark at 4°C in PBS/2% FCS. For extracellular staining, $CD8^+$ T cells were incubated with Abs for 30min on ice.

Ex vivo re-stimulation of splenocytes

Splenocytes from LCMV clone13-infected mice were isolated and incubated with LCMV-GP33 peptide (0.4µg/mL) for 5h at 37°C in the presence of CD107a/b Ab. Subsequently, cells were harvested, washed and stained with the phospho-RPS6$^{Ser235/236}$ (Cell Signaling) anti-IFNγ and anti-TNFα Abs (BD) using Cytofix/Cytoperm (BD) according to manufacturer's recommendations. Analysis was performed by using FlowJo software (Tree Star). Clones of antibodies used are shown in Table S1.

CD8$^+$ T cell Isolation, Activation and Proliferation Assay

CD8$^+$ T-cells from peripheral lymph nodes and spleens of C57BL/6J male mice (bred in the mouse facility of Medical University of Vienna) were purified by negative depletion (purity>90%) and labeled with cell-proliferation dye eFluor450 (eBioscience) as recommended by the manufacturer, activated *in vitro* with plate-bound anti-CD3 (1µg/ml) and anti-CD28 (3µg/ml) Ab and expanded in RPMI1640 medium containing 10% fetal calf serum, GlutaMAX (2mM, ThermoFisher), β-mercaptoethanol (50µM, ThermoFisher) and Penicillin-Streptomycin (ThermoFisher). To test the impact of bile acids (BAs) on CD8$^+$ T-cell activation and proliferation, culture medium was supplemented ± UDCA or NorUDCA for indicated durations and concentrations. Viability of the cells was monitored by a fixable viability dye eFluor506 (ThermoFisher).

Dilution of cell-proliferation dye was evaluated by flow cytometry (LSRII Fortessa, BD Biosciences).

Calcium Influx

Activated $CD8^+$ T cells were labeled at 37°C for 1h with Indo-1 (ThermoFisher), uncoupled Indo-1 was washed out and the cells further incubated ± NorUDCA for 1h at 37°C. Cells were then washed twice with RPMI medium containing 10% FCS, GlutaMAX, β-mercaptoethanol and antibiotics and resuspended in the same medium ± NorUDCA. Cells were incubated with 2µg biotinylated anti-CD3 Ab in 100µl for 15min at room temperature (RT). Cells were mixed with 400µl of 37°C pre-warmed RPMI-1640 medium ± NorUDCA, baseline ratio of violet to blue (405nm/510nm) was measured on a BD-LSR II (Becton Dickinson) flow cytometer for 1 min. 5 µg streptavidin was added to cross-link the TCR. Calcium influx was measured based on the change in the ratio of violet to blue fluorescence for additional 7min. Maximal Calcium flux was induced by addition of Ionomycin (Sigma) after the 7min. Calcium data were analyzed using the FlowJo software.

Lactate Measurements

Supernatants and cells were collected from murine $CD8^+$ T-cell culture ± NorUDCA or Rapamycin upon activation for 24h and processed following the manufacturer's instructions (Cayman). Final concentrations of lactate were

normalized to cell counts.

Phosphatidic Acid (PA) Analysis

Murine $CD8^+$ T cells were activated for 24h ± NorUDCA or Rapamycin and harvested for the measurement of intracellular PA using the fluorometric PicoProbe™ PA Assay Kit (Biovision) following manufacturer's instructions.

Proteomics Sample Preparation and Phosphopeptide Enrichment

Primary murine $CD8^+$ T cells activated with anti-CD3 and anti-CD28 for 24h ± NorUDCA or Rapamycin were harvested in 3 biological replicates for each condition. Each washed cell pellet was lysed separately in 40µL of freshly prepared lysis buffer containing 50mM HEPES (pH8.0), 2% SDS, 0.1M DTT, 1mM PMSF, phosSTOP and protease inhibitor cocktail (Sigma-Aldrich). Samples were rested at RT for 20min before heating to 99°C for 5 min. After cooling down to RT, DNA was sheared by sonication using a Covaris S2 high performance ultrasonicator. Cell debris was removed by centrifugation at 20, 000g for 15min at 20°C. Supernatants were transferred to fresh eppendorf tubes and protein concentration determined using the BCA protein assay kit (Pierce Biotechnology, Rockford, IL). FASP was performed using a 30kDa molecular weight cutoff filter (VIVACON 500; Sartorius Stedim Biotech GmbH, 37, 070 Goettingen, Germany)[2]. In brief, 43µg total proteins per sample were reduced by adding DTT at a final concentration of 83.3mM followed by

incubation at 99°C for 5min. After cooling to room temperature, samples were mixed with 200µL of freshly prepared 8 M urea in 100 mM Tris-HCl (pH 8.5) (UA-solution) in the filter unit and centrifuged at 14, 000g for 15min at 20°C to remove SDS. Any residual SDS was washed out by a second washing step with 200µL of UA. The proteins were alkylated with 100µL of 50mM iodoacetamide in the dark for 30 min at RT. Afterward, three washing steps with 100µL of UA solution were performed, followed by three washing steps with 100µL of 50mM TEAB buffer (Sigma-Aldrich). Proteins were digested with trypsin at a ratio of 1:50 overnight at 37 °C. Peptides were recovered using 40µL of 50mM TEAB buffer followed by 50 µL of 0.5 M NaCl (Sigma-Aldrich). Peptides were desalted using C18 solid phase extraction spin columns (The Nest Group, Southborough, MA). After desalting, peptides were labeled with TMT 10plex™ reagents according to the manufacturer (Pierce, Rockford, IL). After quenching of the labeling reaction, labeled peptides were pooled; organic solvent removed in vacuum concentrator and labeled peptides loaded onto a SPE column. Peptides were eluted with 300µL 80% acetonitrile containing 0.1% trifluoroacetic to achieve a final peptide concentration of ~1 µg/µl. Eluate was then used for phosphopeptide enrichment applying a modified method of immobilized metal affinity chromatography (IMAC)[3]. Briefly, two times 100µL of Ni-NTA superflow slurry (QIAGEN Inc., Valencia, USA) were washed with LCMS-grade water and Ni^{2+} stripped off the beads by incubation with 100mM of EDTA, pH8 solution for 1h at RT. Stripped NTA resin was recharged with $Fe3^{+}$

ions by incubation with a fresh solution of Fe(III)Cl3 and 100µL of charged resin slurry used for the enrichment of a total of ~400 µg TMT-labeled peptides. The unbound fraction was transferred to a fresh glass vial and used for offline fractionation for the analysis of the whole proteome. After washing the slurry with 0.1% TFA, phosphopeptides were eluted with a freshly prepared ammonia solution containing 3mM EDTA, pH8 and all used for offline fractionation for the analysis of the phophoproteome.

Offline Fractionation via RP-HPLC at High pH

Tryptic peptides were re-buffered in 20mM ammonium formiate buffer shortly before separation by reversed phase liquid chromatography at pH10. The unbound fraction of the phosphopeptide enrichment was separated into 96 time-based fractions on a Phenomenex column (150×2.0 mm Gemini-NX 3µm C18 110Å, Phenomenex, Torrance, CA, USA) using an Agilent 1200 series HPLC system fitted with a binary pump delivering solvent at 100µL/min. Acidified fractions were consolidated into 40 fractions via a concatenated strategy[4]. The bound fraction containing the phosphopeptides was separated into 20 fractions on a Dionex column (500µm × 50mm PepSwift RP, monolithic, Dionex Corporation, Sunnyvale, CA, USA) using an Agilent 1, 200 series nanopump delivering solvent at 4µL/min. Peptides were separated by applying a gradient of 90% aceonitrile containing 20mM ammonium formiate, pH10[5]. After solvent removal in a vacuum concentrator, samples were reconstituted in

5% formic acid for LC-MS/MS analysis and kept at -80°C until analysis.

2D-RP/RP Liquid Chromatography Mass Spectrometry

Mass spectrometry was performed on an Orbitrap Fusion Lumos mass spectrometer (ThermoFisher Scientific, San Jose, CA) coupled to an Dionex Ultimate 3000RSLC nano system (ThermoFisher Scientific, San Jose, CA) via nanoflex source interface. Tryptic peptides were loaded onto a trap column (Pepmap 100 5µm, 5×0.3mm, ThermoFisher Scientific, San Jose, CA) at a flow rate of 10µL/min using 2% ACN and 0.1% TFA as loading buffer. After loading, the trap column was switched in-line with a 30cm, 75µm inner diameter analytical column (packed in-house with ReproSil-Pur 120 C18-AQ, 3µm, Dr. Maisch, Ammerbuch-Entringen, Germany). Mobile-phase A consisted of 0.4% formic acid in water and mobile-phase B of 0.4% formic acid in a mix of 90% acetonitrile and 10% water. The flow rate was set to 230 nL/min and a 90 min gradient used (6 to 30% solvent B within 81min, 30 to 65% solvent B within 8min and, 65 to 100% solvent B within 1min, 100% solvent B for 6min before equilibrating at 6% solvent B for 18min). Analysis was performed in a data-dependent acquisition mode. Full MS scans were acquired with a scan range of 375-1650 m/z in the orbitrap at a resolution of 120,000 (at 200Th). Automatic gain control (AGC) was set to a target of $2x10^5$ and a maximum injection time of 50ms. Precursor ions for MS2 analysis were selected using a TopN dependent scan approach with a max cycle time of 3sec. MS2 spectra were

acquired in the orbitrap (FT) at a resolution of 50,000 (at 200Th). Precursor isolation in the quadrupole was set to 1Da and higher energy collision induced dissociation (HCD) with normalized collision energy (NCE) of 38%. AGC was set to $5x10^4$ with a maximum injection time of 54ms and 150ms for the proteome and phosphoproteome, respectively. Dynamic exclusion for selected ions was 60s for the proteome and 30s for the phosphoproteome. A single lock mass at m/z 445.120024 for recalibration was employed[6]. Xcalibur version 4.0.0 and Tune 2.1 were used to operate the instrument. Phosphoproteomics samples were acquired in two technical replicates.

Proteomics and Phosphoproteomics Data Analysis

Acquired raw data files were processed using the Proteome Discoverer 2.2.0. platform, utilizing the Sequest HT database search engine and Percolator validation software node (V3.04) to remove false positives with a false discovery rate (FDR) of 1% on peptide and protein level under strict conditions. Searches were performed with full tryptic digestion against the mouse SwissProt database v2017.12 appended with known contaminants (25,293 sequences) with up to two miscleavage sites. Oxidation (+15.9949 Da) of methionine, deamidation (+0.984Da) of glutamine and asparagine, and protein N-termini acetylation (+42.011Da) were set as variable modifications, whilst carbamidomethylation (+57.0214Da) of cysteine residues and TMT 6-plex labeling of peptide N-termini and lysine residues were set as fixed modifications.

For phosphopeptides phosphorylation (+79.966Da) of serine, threonine and tyrosine was additionally included as a variable modification. Data was searched with mass tolerances of ±10ppm and 0.025Da on the precursor and fragment ions, respectively. Results were filtered to include peptide spectrum matches with Sequest HT cross-correlation factor scores of ≥1 and 1% FDR peptide confidence. The ptmRS algorithm was additionally used to validate phospopeptides with a set score cutoff of 90. PSMs with precursor isolation interference values of ≥ 50% and average TMT-reporter ion signal-to-noise values ≤ 10 were excluded from quantitation. Isotopic impurity correction and TMT channel-normalization based on total peptide amount were applied. Protein abundances were further normalized to equal median in each TMT channel. One-way ANOVA test corrected for false discovery rate by Benjamini–Hochberg procedure followed by Tukey post-hoc test was used to calculate statistical significance of comparisons made among 3 groups of observed changes on protein level. In cases where only the data on NorUDCA and control samples were compared the statistical significance was calculated by paired Student's t-test. TMT ratios with *P*-values < 0.01 were considered as significant. For the phosphopeptide analysis, peptides that were changing in opposite directions in the two technical replicates were discarded, moreover Student's t-test was performed on each technical replicate separately and *P*-value was required to be lower than 0.01 in both replicates in order to consider phosphopeptide abundance change as significant. The mean abundance of

each biological replicate from the two technical replicates was calculated and further normalized to their corresponding proteome abundance.

Human T cell experiments

3 independent experiments with peripheral T-cells obtained from PSC patients (also suffering from associated inflammatory bowel disease) and age and gender matched healthy volunteers were performed in parallel following the Declaration of Helsinki and approved by the Ethics Committee of the MUV (747/2011 and 2001/2018). Bulk T-cells from peripheral blood mononuclear cells (PBMCs) were isolated by negative depletion[7], labeled with 1μM CFSE and rested overnight in RPMI 1640 medium with 5% heat-inactivated FCS, 2mM L-glutamine, 100μg/ml streptomycin and 100U/ml penicillin. T-cells were activated with plate-bound anti-CD3 (1μg/ml) plus soluble anti-CD28 (0.5μg/ml) Abs ± NorUDCA or UDCA or Rapamycin. Lymphoblastogenesis, proliferation and activity of mTORC1 and Erk1/2 were assessed on day3 on a Fortessa flow cytometer (BD Biosciences)[7].

Supplementary figures

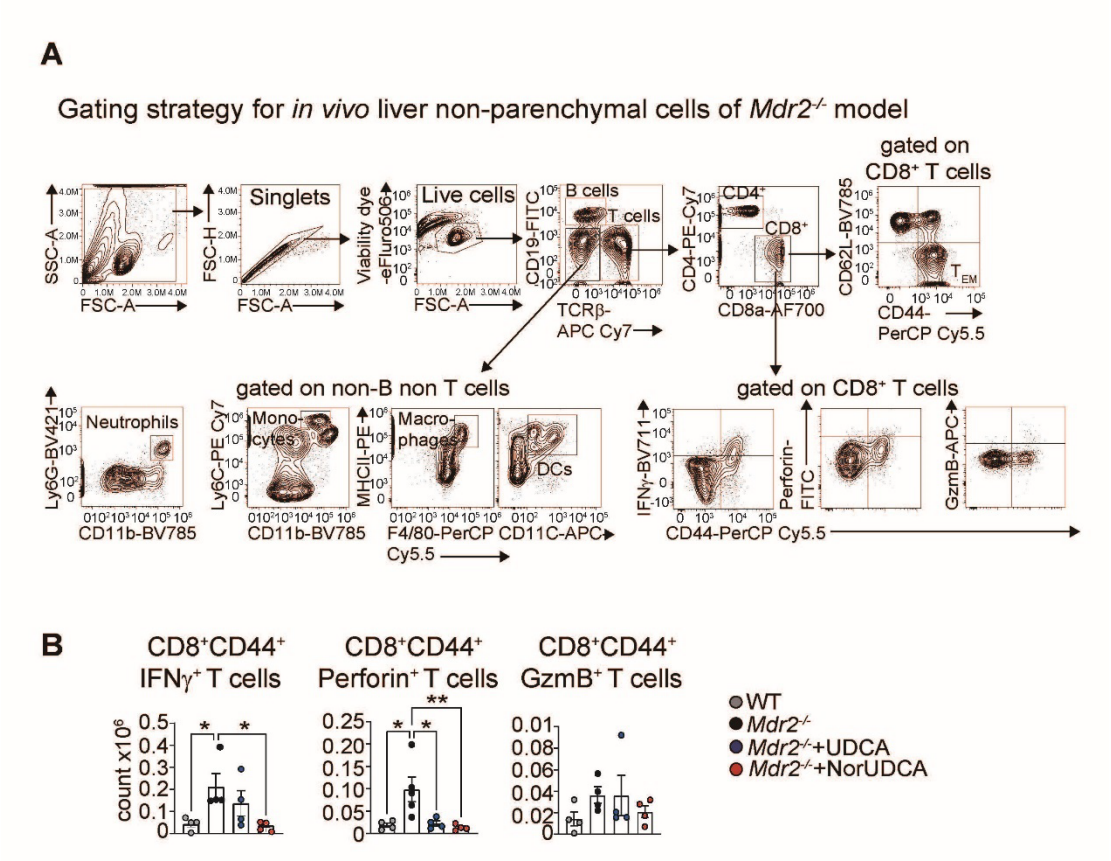

Fig. S1. Gating strategy for *in vivo* liver non-parenchymal cells of *Mdr2*$^{-/-}$ model and impact of NorUDCA on number of cytokine- expressing hepatic CD8^{+} T-cells. (A) Gating strategy for flow cytometry analysis in vivo liver non-parenchymal cells of *Mdr2*$^{-/-}$ model. (B) Quantitative analysis of hepatic CD8^{+} T-cells expressing cytokines of indicated groups. Data are representative of 2 independent-experiments. 4 biologically independent-animals were used per group during experiments. Quantitative data are presented as mean±SE. *P*-values were calculated by one-way ANOVA corrected for multiple comparisons with Dunnett test using *Mdr2*$^{-/-}$ mice as reference. *=*P*<0.05, **=*P*<0.01. GrzmB, GranzymeB.

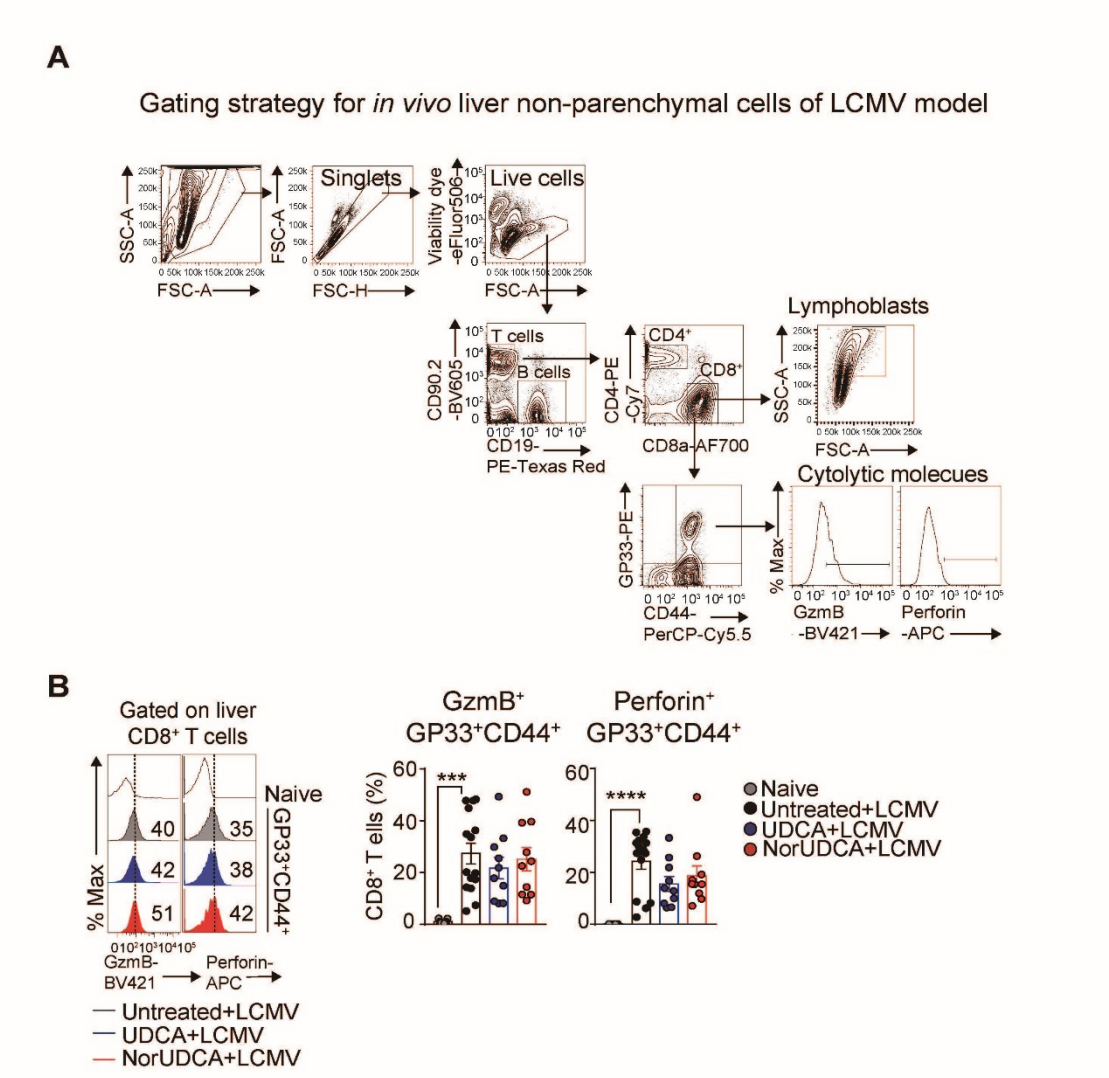

Fig. S2. Gating strategy for liver non-parenchymal cells of *in vivo* LCMV Clone 13 model and NorUDCA impact on hepatic CD8⁺ T-cell cytolytic molecule expression. (A) Gating strategy for flow cytometry analysis of liver non-parenchymal cells of *in vivo* LCMV Clone 13 model. (B) Representative plots of intrahepatic virus-specific CD8⁺ expressing cytolytic molecules. Data are summary of 3 independent-experiments. At least 3 biologically independent-animals were used per group during experiments. Quantitative data are presented as mean±SE. *P*-values were calculated by one-way ANOVA corrected with Tukey post-hoc test. Cells recognizing the GP33 peptide in the

context of MHC class I presentation are labeled as GP33^{+}. ***=*P*<0.001, ***=*P*<0.001, ****=*P*<0.0001. GrzmB, GranzymeB.

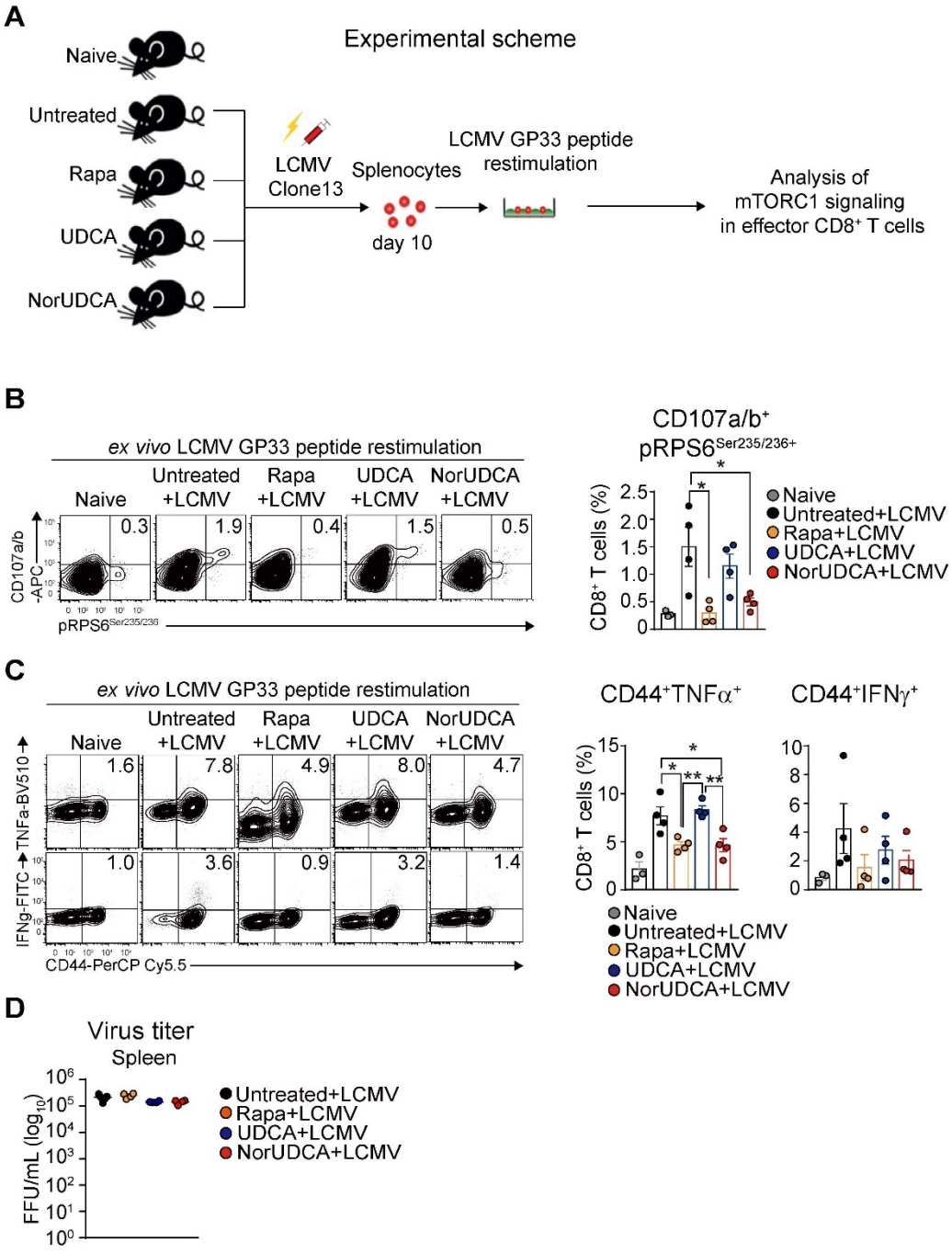

Fig. S3. Splenic CD8⁺ T-cells from NorUDCA treated LCMV mice show reduced mTORC1 and ameliorated TNFα expression but unaltered IFNγ expression upon *ex vivo* re-stimulation with GP33-LCMV peptide. (A) Experimental scheme. (B) pRPS6$^{Ser235/236}$ expression in *ex vivo* isolated splenic CD107a/b⁺CD8⁺ T-cells (i.e. cells that are true effectors and degranulated)

upon GP33 LCMV peptide re-stimulation. Quantitative analysis is shown alongside. (C) TNFα or IFNγ expression on gated splenic CD107a/b^{+}CD8^{+} T-cells isolated from indicated groups upon *ex vivo* LCMV GP33 peptides re-stimulation. Quantitative analysis is shown alongside. (D) Spleen LCMV virus titer. Data is representative of 2 independent-experiments. At least 3 biological independent-animals were used per group during experiment. Summary data are presented as mean±SE. *P*-values were calculated by one-way ANOVA corrected with Tukey post-hoc test. *=$P<0.05$, **=$P<0.01$. Rapa, Rapamycin.

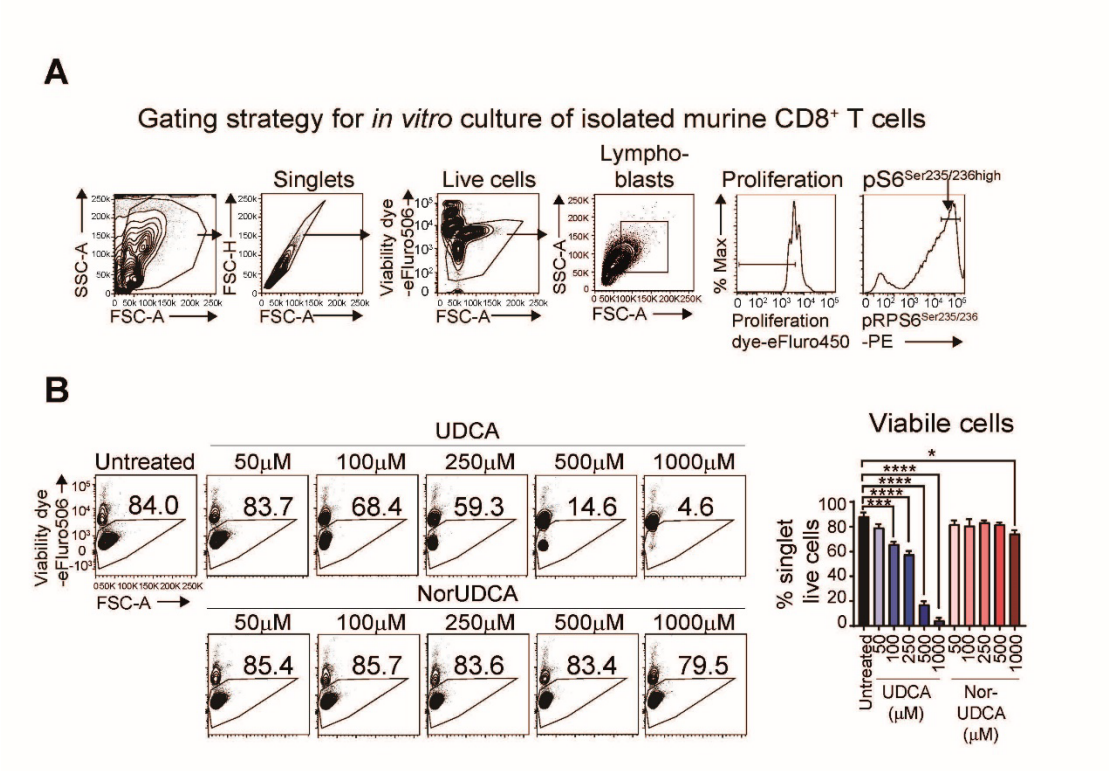

Fig. S4. Gating strategy and titration assay for *in vitro* culture of primary murine CD8⁺ T-cells. (A) Gating strategy for flow cytometry analysis of *in vitro* culture of primary murine CD8⁺ T-cells. (B) Titration assay of *in vitro* culture of primary murine CD8⁺ T-cells activated ± NorUDCA or UDCA at various concentrations for 24h. Summary data of 2 independent-experiments are presented as mean±SE. *P*-values were calculated by one-way ANOVA corrected with Tukey post-hoc test, untreated group was used as reference for comparison. *=*P*<0.05, **=*P*<0.01, ***=*P*<0.001, ****=*P*<0.0001.

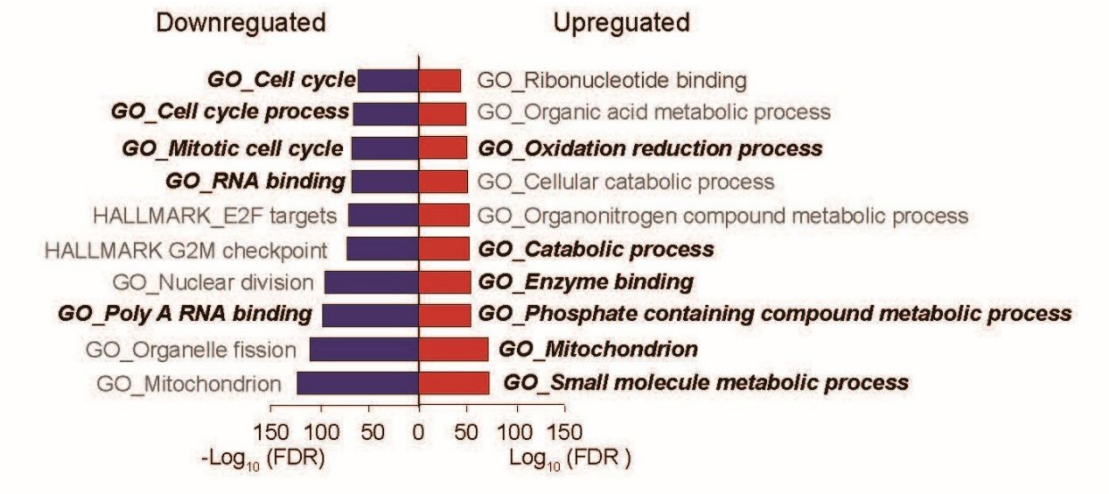

Fig. S5. The top 10 enriched pathways for significantly up- and downregulated proteins by NorUDCA in activated CD8⁺ T-cells. The top 10 enriched Hallmark, Gene Ontology (GO), KEGG pathways for significantly up- and downregulated proteins by NorUDCA. Overlap of top 10 enriched pathways modulated by NorUDCA and Rapamycin are shown in bold, black and italic. Pathways uniquely modulated by NorUDCA are shown in grey, regular.

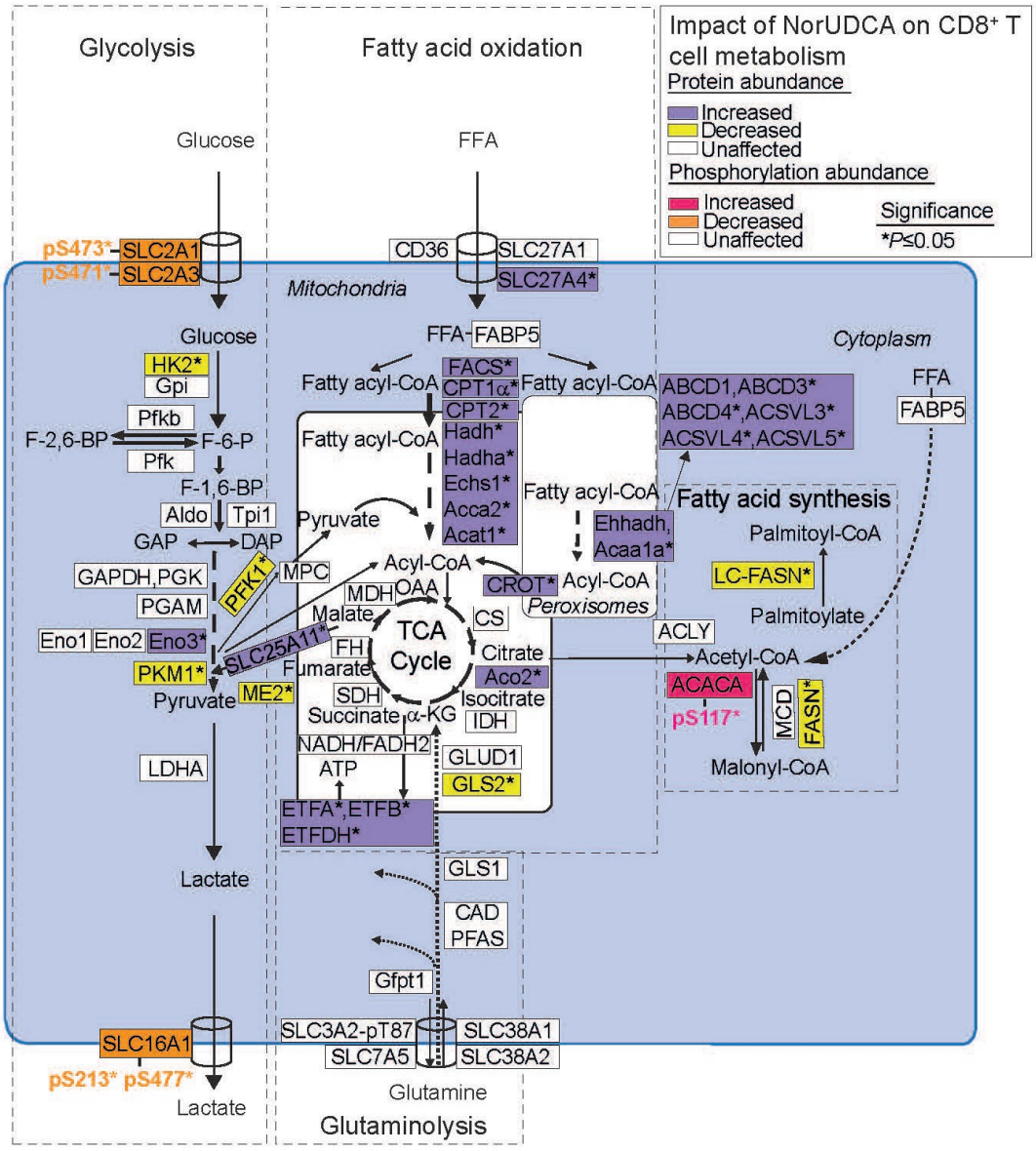

Fig. S6. NorUDCA reduces glycolysis while enhancing fatty acid oxidation machinery in activated CD8⁺ T-cells. Schematic summary of key phosphoproteomics data showing the impact of NorUDCA on glycolysis and fatty acid oxidation pathways. Figure shows protein, protein phosphorylation and genes affected by NorUDCA. The color code was inserted for direction of changes. Data were obtained from 3 independent-experiments. *P*-values were calculated with two tailed, paired student's t test between untreated and NorUDCA-treated groups. *=*P*<0.05.

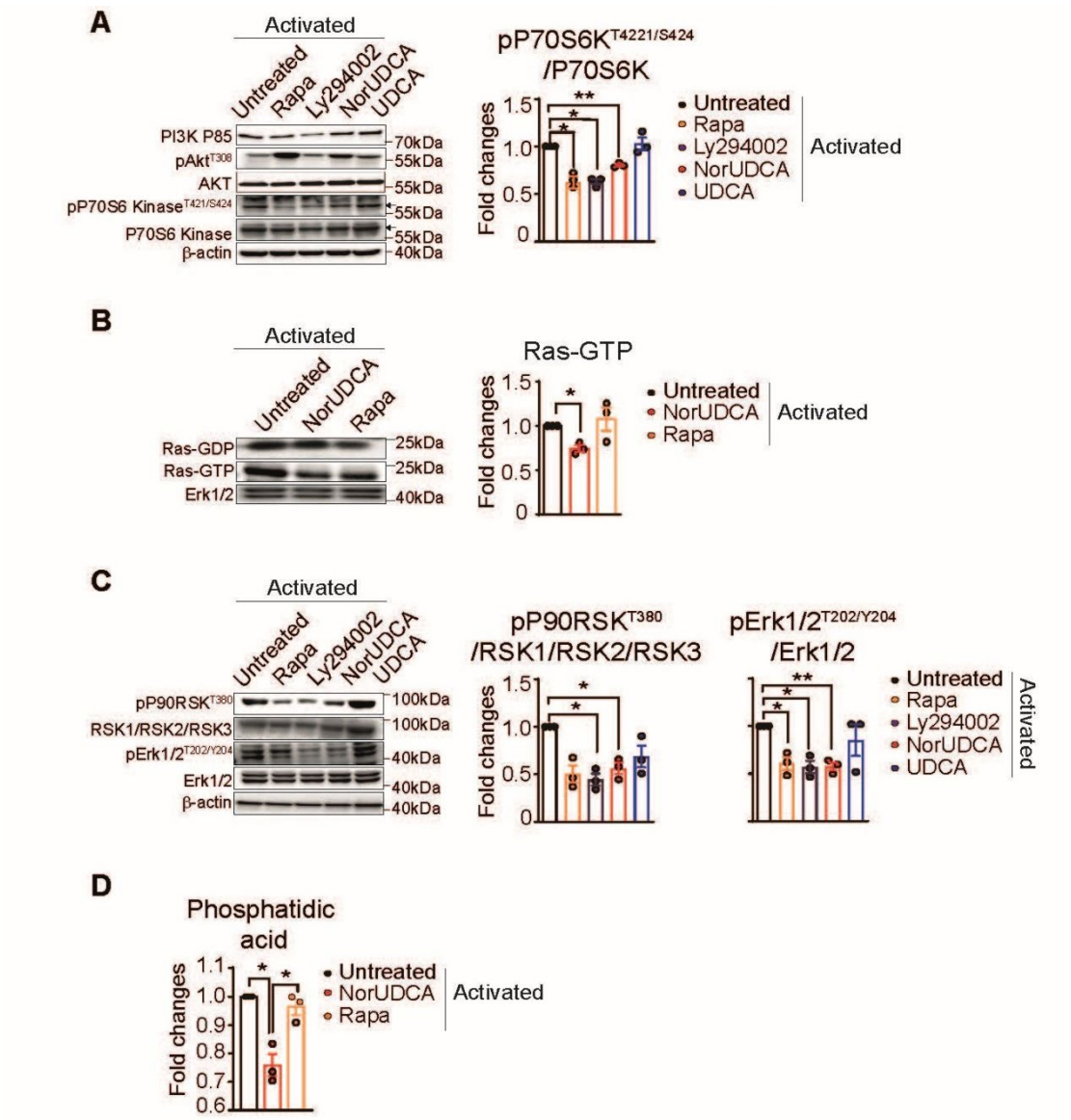

Fig. S7. NorUDCA attenuates Ras-Erk-P90RSK-mTORC1 signaling and reduces intracellular PA level in activated CD8⁺ T-cells. (A-C) Representative immunoblots of Ras-Erk-P90RSK-mTORC1 pathway in murine CD8⁺ T-cells activated for 24h. Quantitative analysis is shown alongside. (D) Intracellular PA of CD8⁺ T-cells activated for 24h stimulated under indicated conditions. Data are representative of 3 independent-experiments. Quantitative data are presented as mean±SE. *P*-values were calculated by one-way ANOVA corrected with Tukey post-hoc test. Data are normalized to protein abundance

of untreated group. *=P<0.05, **=P<0.01. Rapa, Rapamycin; PA, phosphatidic acid.

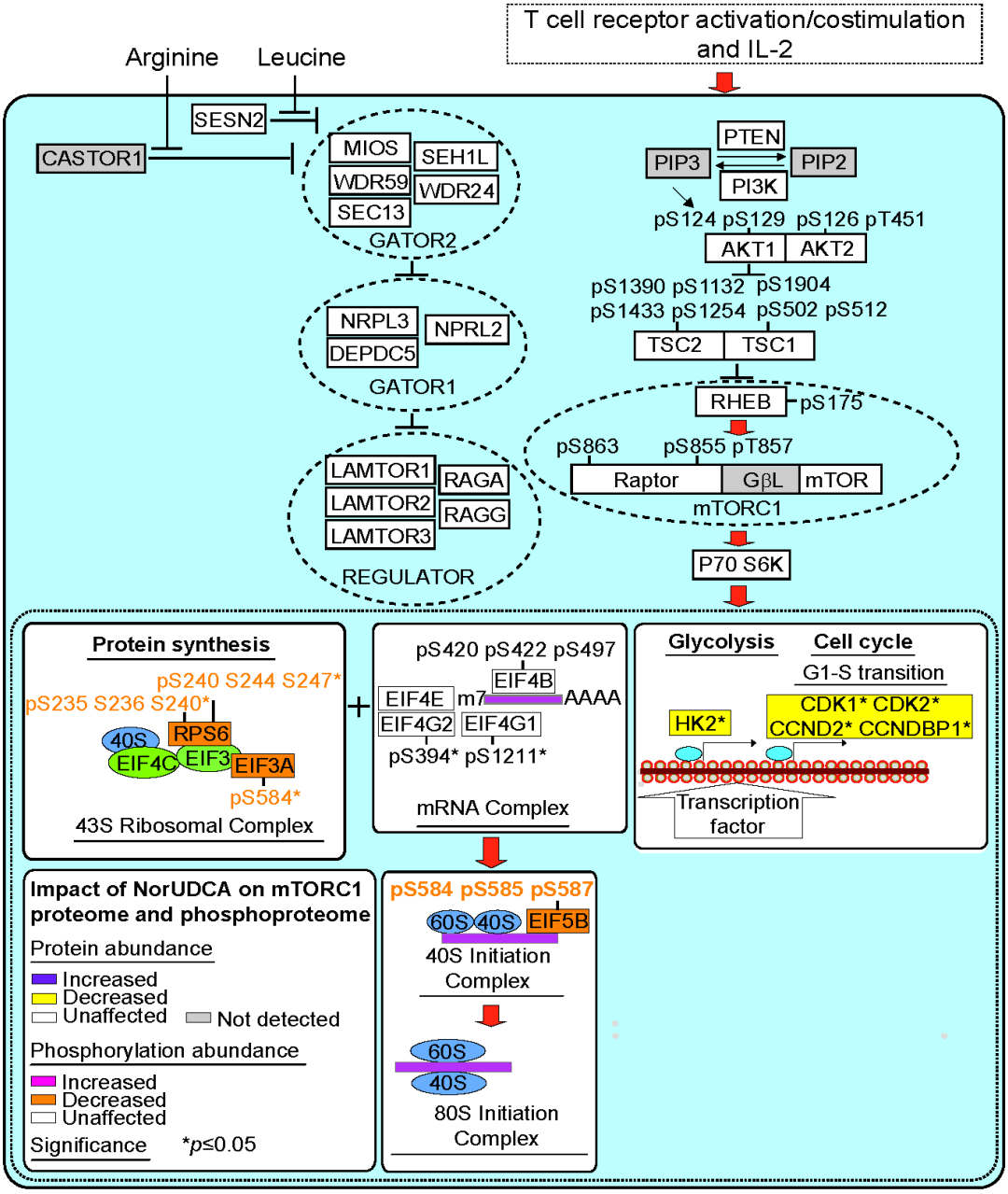

Fig. S8. NorUDCA modulation of CD8⁺ T-cell mTORC1 proteome and phosphoproteome. Schematic overview of mTORC1 signaling and down-stream pathways affected by NorUDCA. Color code was inserted for direction of changes. Data were obtained from 3 independent-experiments. Abundance of phosphoproteins were normalized to the relevant total abundance of protein. *P*-values were calculated with two-tailed paired Student's t test between

untreated and NorUDCA groups. *= P<0.05.

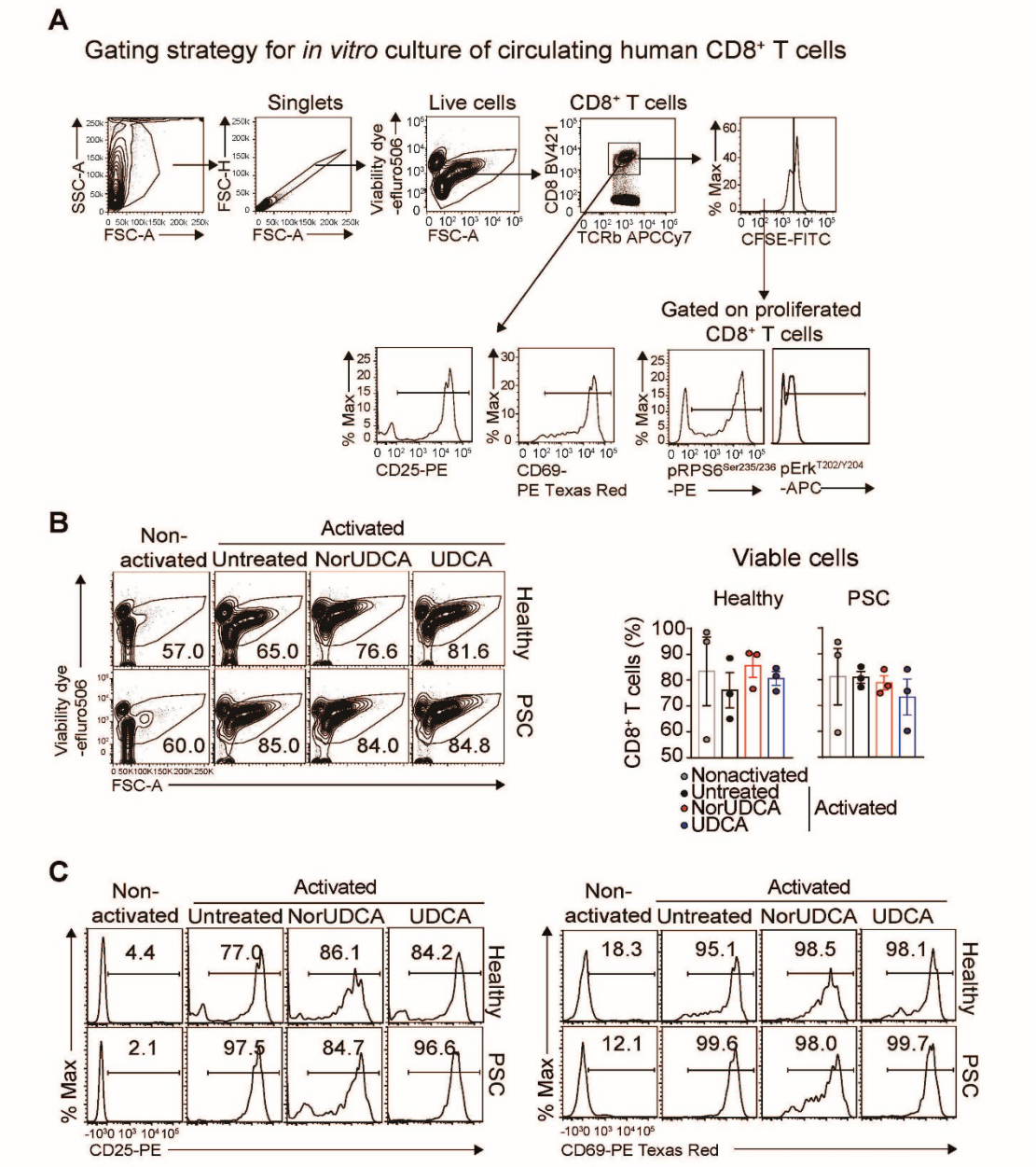

Fig. S9. NorUDCA does not affect human CD8⁺ T-cell viability and activation. (A) Gating strategy for flow cytometry analysis of *in vitro* culture of circulating human CD8⁺ T-cells. (B) Viability profile of circulating CD8⁺ T-cells from peripheral blood of healthy volunteer and PSC patients treated as indicated for 3 days. Quantitative analysis of 3 independent experiments is shown alongside. (C) Expression of CD25 and CD69 on live singlet CD8⁺ T-cells of healthy volunteer and PSC patient are shown. Data in (B,C) are

representative of 3 independent-experiments. *P*-values were calculated by one-way ANOVA corrected with Tukey post-hoc test. PSC, primary sclerosing cholangitis; Rapa, Rapamycin.

Table S1. Antibodies used in the study.

Antigen	Clone	Company	Application
CD4	RM4-5	Biolegend	F.C.
CD8a	53-6.7	Biolegend	F.C.
CD11b	M1/70	Biolegend	F.C.
CD11c	N418	Biolegend	F.C.
CD45R	B220; RA3-6B2	Biolegend	F.C.
Gr1	RB6-8C5	Biolegend	F.C.
Ter-119	TER-119	Biolegend	F.C.
NK1.1	PK136	Biolegend	F.C.
CD25	PC61	Biolegend	F.C.
CD69	H1.2F3	Biolegend	F.C.
CD62L	MEL-14	Biolegend	F.C.
CD8a	SK1	Biolegend	F.C.
CD4	SK3	Biolegend	F.C.
CD69	FN50	Biolegend	F.C.
CD25	BC96	Biolegend	F.C.
Perforin	eBioOMAK-D	Thermofisher	F.C.
TCRa/b	IP26	Biolegend	F.C.
Granzyme B	GB11	BD Biosciences	F.C.
INFγ	XMG1.2	BD Biosciences	F.C.
TNFα	MP6-XT22	BD Biosciences	F.C.
CD3	145-2C11	BD Biosciences	F.C.
CD28	37.51	BD Biosciences	F.C.
CD3	OKT3	BD Biosciences	F.C.
CD28	CD28.2	BD Biosciences	F.C.
GLUT1	EPR3915	Abcam	F.C.
CD3	SP7	Novus	I.F.
CD8	53-6.7	Novus	I.F.
Rabbit IgG	Polyclonal	Invitrogen	I.F.
pmTOR(Ser2448)	D9C2	Cell Signaling Technology	I.B.
mTOR	Polyclonal	Cell Signaling Technology	I.B.
pP70S6 Kinase (T421/S424)	Polyclonal	Cell Signaling Technology	I.B.
P70S6 Kinase	Polyclonal	Cell Signaling Technology	I.B.
AKT	Polyclonal	Cell Signaling Technology	I.B.
Beta-actin	8H10D10	Cell Signaling Technology	I.B.
PI3 Kinase p85	Polyclonal	Cell Signaling Technology	I.B.
pAkt (Thr308)	D25E6	Cell Signaling Technology	I.B.

pP90RSK(T380)	D3H11	Cell Signaling Technology	I.B.
RSK1/RSK2/RSK3	32D7	Cell Signaling Technology	I.B.
pP44/42 MAPK(Erk1/2)(T202/Y204)	D13.14.4E	Cell Signaling Technology	I.B
p44/42 MAPK (Erk1/2)		Cell Signaling Technology	I.B
Perforin	S16009A	Biolegend	F.C.
CD107a	1D4B	Biolegend	F.C.
CD107b	M3184	Biolegend	
CD44	IM7	Biolegend	F.C.
CD19	6D5	Biolegend	F.C.
CD90.2	30-H12	Biolegend	F.C.
pRPS6$^{S235/236}$	D57.2.2E	Cell Signaling Technology	F.C.
pRPS6$^{S240/244}$	D68F8	Cell Signaling Technology	F.C.
pP44/42 MAPK(Erk1/2)(T202/Y204)	E10	Cell Signaling Technology	F.C.

Abbreviations: F.C., Flow Cytometry; I.B., Immunoblotting; I.F., Immunofluorescence.

Table S2. Primer sequences used in the study.

Gene	**Forward** (5' - 3')	**Reverse** (5' - 3')
qRTPCR		
Hprt	GATACAGGCCAGACTTTGTTG	GGTAGGCTGGCCTATAGGCT
Hk2	GGCTAGGAGCTACCACACAC	AACTCGCCATGTTCTGTCCC
Slc16a3	GACGAGTAGGCTGGACTGAA	GCTGCTTTCACCAAGAACTGA
Ldha	ATGAGTAAGTCCTCAGGCGG	GGACTTTGAATCTTTTGAGACCTTG
Cpt1a	TGAGTGGCGTCCTCTTTGG	CAGCGAGTAGCGCATAGTCA

Table S3. Proteins involved in the GO_Mitochondria pathways upregulated and downregulated by NorUDCA.

Proteins modulated by NorUDCA in downregulation of Mitochoria pathways	
Protein name	Discription
TP53	tumor protein p53
DNA2	DNA replication helicase/nuclease 2
AKAP8	A-kinase anchoring protein 8
PNPT1	polyribonucleotide nucleotidyltransferase 1
TYMS	thymidylate synthetase
DHFR	dihydrofolate reductase
CDK1	cyclin dependent kinase 1
DLGAP5	DLG associated protein 5
RAD51	RAD51 recombinase
MSTO1	misato mitochondrial distribution and morphology regulator 1
TFDP1	transcription factor Dp-1
GADD45GIP 1	GADD45G interacting protein 1
PIN1	"peptidylprolyl cis/trans isomerase, NIMA-interacting 1
HAUS3	HAUS augmin like complex subunit 3
NME6	NME/NM23 nucleoside diphosphate kinase 6
AKT1	AKT serine/threonine kinase 1
GADD45GIP 1	GADD45G interacting protein 1
PIN1	"peptidylprolyl cis/trans isomerase, NIMA-interacting 1
HAUS3	HAUS augmin like complex subunit 3
NME6	NME/NM23 nucleoside diphosphate kinase 6
AKT1	AKT serine/threonine kinase 1
RPS3	ribosomal protein S3
TOP3A	DNA topoisomerase III alpha
SLC25A33	solute carrier family 25 member 33
MYO19	myosin XIX
MRPL41	mitochondrial ribosomal protein L41
HJURP	Holliday junction recognition protein
CASP8AP2	Caspase 8 assciate protein 2
CDK5RAP1	CDK5 regulatory subunit associated protein 1
CRY1	cryptochrome circadian regulator 1
APEX2	apurinic/apyrimidinic endodeoxyribonuclease 2
DAP3	death associated protein 3
NSUN4	NOP2/Sun RNA methyltransferase 4

MTERF4	mitochondrial transcription termination factor 4
TRMT10C	tRNA methyltransferase 10C, mitochondrial RNase P subunit
MRPS9	mitochondrial ribosomal protein S9
MRPL40	mitochondrial ribosomal protein L40
MRPL11	mitochondrial ribosomal protein L11
MRPL22	mitochondrial ribosomal protein L22
MRPS7	mitochondrial ribosomal protein S7
MRPL58	mitochondrial ribosomal protein L58
MRPL9	mitochondrial ribosomal protein L9
MRPL13	mitochondrial ribosomal protein L13
MRPS18A	mitochondrial ribosomal protein S18A
MRPL15	mitochondrial ribosomal protein L15
MRPL3	mitochondrial ribosomal protein L3
MRPL28	mitochondrial ribosomal protein L28
MRPL54	mitochondrial ribosomal protein L54
MRPL2	mitochondrial ribosomal protein L2
MRPL4	mitochondrial ribosomal protein L4
MRPL37	mitochondrial ribosomal protein L37
MRPL27	mitochondrial ribosomal protein L27
MRPL32	mitochondrial ribosomal protein L32
MRPL45	mitochondrial ribosomal protein L45
MRPS21	mitochondrial ribosomal protein S21
MRPS14	mitochondrial ribosomal protein S14
MRPS5	mitochondrial ribosomal protein S5
MRPL1	mitochondrial ribosomal protein L1
YARS2	tyrosyl-tRNA synthetase 2
AARS2	alanyl-tRNA synthetase 2, mitochondrial
ERAL1	Era like 12S mitochondrial rRNA chaperone 1
GFM2	G elongation factor mitochondrial 2
TUFM	Tu translation elongation factor, mitochondrial
GFM1	G elongation factor mitochondrial 1
RCC1L	RCC1 like
NOA1	nitric oxide associated 1
MTIF2	mitochondrial translational initiation factor 2
TRUB2	TruB pseudouridine synthase family member 2
FASTKD2	FAST kinase domains 2
NGRN	neugrin, neurite outgrowth associated
PTCD3	pentatricopeptide repeat domain 3
MTIF3	mitochondrial translational initiation factor 3
TEFM	transcription elongation factor, mitochondrial
FASTKD5	FAST kinase domains 5
POLRMT	RNA polymerase mitochondrial
CD3EAP	CD3e molecule associated protein

HSPD1	heat shock protein family D (Hsp60) member 1
LGALS3	galectin 3
SLIRP	SRA stem-loop interacting RNA binding protein
KARS1	lysyl-tRNA synthetase 1
FARS2	"phenylalanyl-tRNA synthetase 2, mitochondrial
IREB2	iron responsive element binding protein 2
ASS1	argininosuccinate synthase 1
DDX28	DEAD-box helicase 28
TRMU	tRNA 5-methylaminomethyl-2-thiouridylate methyltransferase
MTPAP	mitochondrial poly(A) polymerase\
MRM3	mitochondrial rRNA methyltransferase 3
GRSF1	G-rich RNA sequence binding factor 1
PTCD1	pentatricopeptide repeat domain 1
KYAT3	kynurenine aminotransferase 3
PTCD2	pentatricopeptide repeat domain 2
AKAP1	A-kinase anchoring protein 1
MAPK8	mitogen-activated protein kinase 8
DCTPP1	dCTP pyrophosphatase 1
MRPL19	mitochondrial ribosomal protein L19
MRPL17	mitochondrial ribosomal protein L17
MRPL47	mitochondrial ribosomal protein L47
MRPL57	mitochondrial ribosomal protein L57
MRPL24	mitochondrial ribosomal protein L24
MRPL33	mitochondrial ribosomal protein L33
MRPL53	mitochondrial ribosomal protein L53
MRPL48	mitochondrial ribosomal protein L48
MRPL38	mitochondrial ribosomal protein L38
MRPS22	mitochondrial ribosomal protein S22
MRPS33	mitochondrial ribosomal protein S33
TARS2	"threonyl-tRNA synthetase 2, mitochondrial
HARS1	histidyl-tRNA synthetase 1
QRSL1	glutaminyl-tRNA amidotransferase subunit QRSL1
MTG1	mitochondrial ribosome associated GTPase 1
MTERF3	mitochondrial transcription termination factor 3
DHODH	dihydroorotate dehydrogenase (quinone)
BNIP3	BCL2 interacting protein 3
MTFR2	mitochondrial fission regulator 2
GSK3A	glycogen synthase kinase 3 alpha
GLRX2	glutaredoxin 2
TIGAR	TP53 induced glycolysis regulatory phosphatase
MARS2	methionyl-tRNA synthetase 2, mitochondrial
METTL17	methyltransferase like 17
THOP1	thimet oligopeptidase 1

NLN	neurolysin
FPGS	folylpolyglutamate synthase
PDHB	pyruvate dehydrogenase E1 beta subunit
DEGS1	delta 4-desaturase, sphingolipid 1
NMNAT3	nicotinamide nucleotide adenylyltransferase 3
KIF1B	kinesin family member 1B
RAF1	Raf-1 proto-oncogene, serine/threonine kinase
STING1	stimulator of interferon response cGAMP interactor 1
PI4KB	phosphatidylinositol 4-kinase beta
RIPK3	receptor interacting serine/threonine kinase 3
SPATA5	spermatogenesis associated 5
RIPK2	receptor interacting serine/threonine kinase 2
MMAA	metabolism of cobalamin associated A
GTPBP3	GTP binding protein 3, mitochondrial
PPIF	peptidylprolyl isomerase F
SDHAF2	succinate dehydrogenase complex assembly factor 2
GLS	glutaminase
TMLHE	trimethyllysine hydroxylase, epsilon
NDUFB8	NADH:ubiquinone oxidoreductase subunit B8
NUDT9	nudix hydrolase 9
COQ5	coenzyme Q5, methyltransferase
NDUFAF7	NADH:ubiquinone oxidoreductase complex assembly factor 7
PDSS2	decaprenyl diphosphate synthase subunit 2
MPST	mercaptopyruvate sulfurtransferase
PITRM1	pitrilysin metallopeptidase 1
ME2	malic enzyme 2
ALDH1B1	aldehyde dehydrogenase 1 family member B1
GCAT	glycine C-acetyltransferase
QTRT1	queuine tRNA-ribosyltransferase catalytic subunit 1
RBFA	ribosome binding factor A
COX7A2L	cytochrome c oxidase subunit 7A2 like
CIAPIN1	cytokine induced apoptosis inhibitor 1
ACAT2	acetyl-CoA acetyltransferase 2
TAMM41	TAM41 mitochondrial translocator assembly and maintenance homolog
MT-CO2	mitochondrially encoded cytochrome c oxidase II
SLC25A13	solute carrier family 25 member 13
BLOC1S2	biogenesis of lysosomal organelles complex 1 subunit 2
FOXRED1	FAD dependent oxidoreductase domain containing 1
NDUFAF2	NADH:ubiquinone oxidoreductase complex assembly factor 2
PISD	phosphatidylserine decarboxylase
L2HGDH	L-2-hydroxyglutarate dehydrogenase
COQ4	coenzyme Q4

GHITM	growth hormone inducible transmembrane protein
CHCHD2	coiled-coil-helix-coiled-coil-helix domain containing 2
PGAM5	"PGAM family member 5, mitochondrial serine/threonine protein phosphatas
FMC1	formation of mitochondrial complex V assembly factor 1 homolog
PTRH2	peptidyl-tRNA hydrolase 2
GZMB	granzyme B
BSG	basigin (Ok blood group)
SACS	sacsin molecular chaperone
KIFBP	kinesin family binding protein

Proteins modulated by NorUDCA in upregulation of Mitochoria pathways	
Protein name	Description
PKM	pyruvate kinase M1/2
IDH1	isocitrate dehydrogenase (NADP(+)) 1
CYB5R3	cytochrome b5 reductase 3
CAT	catalase
ARSB	arylsulfatase B
GSTP1	glutathione S-transferase pi 1
PARK7	Parkinsonism associated deglycase
CPT1A	carnitine palmitoyltransferase 1A
GLUD1	glutamate dehydrogenase 1
MECP2	methyl-CpG binding protein 2
HADH	hydroxyacyl-CoA dehydrogenase
IDH2	isocitrate dehydrogenase (NADP(+)) 2
GLUL	glutamate-ammonia ligase
ACSL4	acyl-CoA synthetase long chain family member 4
OXCT1	3-oxoacid CoA-transferase 1
ABCD3	ATP binding cassette subfamily D member 3
ALDH18A1	aldehyde dehydrogenase 18 family member A1
ADH5	alcohol dehydrogenase 5 (class III), polypeptide
ACAT1	acetyl-CoA acetyltransferase 1
PYCR1	pyrroline-5-carboxylate reductase 1
SLC25A12	solute carrier family 25 member 12
HADHB	hydroxyacyl-CoA dehydrogenase trifunctional multienzyme complex subunit beta
SCP2	sterol carrier protein 2
ACADL	acyl-CoA dehydrogenase long chain
HADHA	hydroxyacyl-CoA dehydrogenase trifunctional multienzyme complex subunit alpha
ACSS1	acyl-CoA synthetase short chain family member 1

SUCLG2	succinate-CoA ligase GDP-forming beta subunit
SUCLA2	succinate-CoA ligase ADP-forming beta subunit
ECH1	enoyl-CoA hydratase 1
ACAA2	acetyl-CoA acyltransferase 2
HSD17B10	hydroxysteroid 17-beta dehydrogenase 10
IVD	isovaleryl-CoA dehydrogenase
ETFA	electron transfer flavoprotein subunit alpha
ACADS	acyl-CoA dehydrogenase short chain
ECHS1	enoyl-CoA hydratase, short chain 1
ECI1	enoyl-CoA delta isomerase 1
ALDH7A1	aldehyde dehydrogenase 7 family member A1
MTHFD2	methylenetetrahydrofolate dehydrogenase (NADP+ dependent) 2, methenyltetrahydrofolate cyclohydrolase
SUCLG1	succinate-CoA ligase alpha subunit
COQ9	coenzyme Q9
FXN	frataxin
GARS1	glycyl-tRNA synthetase 1
PON2	paraoxonase 2
GSTZ1	glutathione S-transferase zeta 1
MMUT	methylmalonyl-CoA mutase
KYAT1	kynurenine aminotransferase 1
RIDA	reactive intermediate imine deaminase A homolog
ACSL5	acyl-CoA synthetase long chain family member 5
GNPAT	glyceronephosphate O-acyltransferase
PCCA	propionyl-CoA carboxylase subunit alpha
PCCB	propionyl-CoA carboxylase subunit beta
PCK2	phosphoenolpyruvate carboxykinase 2, mitochondrial
AARS1	alanyl-tRNA synthetase 1
MCCC2	methylcrotonoyl-CoA carboxylase 2
MTHFS	methenyltetrahydrofolate synthetase
EARS2	"glutamyl-tRNA synthetase 2, mitochondrial
HIBCH	3-hydroxyisobutyryl-CoA hydrolase
PPA2	inorganic pyrophosphatase 2
PDE2A	phosphodiesterase 2A
PARP1	poly(ADP-ribose) polymerase 1
NAXE	NAD(P)HX epimerase
AGPAT4	1-acylglycerol-3-phosphate O-acyltransferase 4
CNP	"2',3'-cyclic nucleotide 3' phosphodiesterase
PNKP	polynucleotide kinase 3'-phosphatase
DTYMK	deoxythymidylate kinase
DGUOK	deoxyguanosine kinase
AK3	adenylate kinase 3
MMAB	metabolism of cobalamin associated B

FOXO1	Forkhead box O1
ATP5PO	ATP synthase peripheral stalk subunit OSCP
ATP5PD	ATP synthase peripheral stalk subunit d
CLYBL	citrate lyase beta like
ISCA2	iron-sulfur cluster assembly 2
SLC25A1	solute carrier family 25 member 1
SFXN3	sideroflexin 3
PYCARD	PYD and CARD domain containing
NCSTN	nicastrin
CAPN1	calpain 1
PPP3CA	protein phosphatase 3 catalytic subunit alpha
CCR7	C-C motif chemokine receptor 7
FYN	"FYN proto-oncogene, Src family tyrosine kinase
BCL2	BCL2 apoptosis regulator
CASP8	caspase 8
STAP1	signal transducing adaptor family member 1
DNAJA3	DnaJ heat shock protein family (Hsp40) member A3
SRI	sorcin
ARL2	ADP ribosylation factor like GTPase 2
SLC25A4	solute carrier family 25 member 4
IDE	insulin degrading enzyme
SOD2	superoxide dismutase 2
RTN4IP1	reticulon 4 interacting protein 1
NDUFA13	NADH:ubiquinone oxidoreductase subunit A13
TRAP1	TNF receptor associated protein 1
NDUFV1	NADH:ubiquinone oxidoreductase core subunit V1
GSTK1	glutathione S-transferase kappa 1
WWOX	WW domain containing oxidoreductase
PRDX5	peroxiredoxin 5
CYCS	cytochrome c, somatic
NDUFA8	NADH:ubiquinone oxidoreductase subunit A8
NDUFS8	NADH:ubiquinone oxidoreductase core subunit S8
NDUFV3	NADH:ubiquinone oxidoreductase subunit V3
NDUFA6	NADH:ubiquinone oxidoreductase subunit A6
NDUFB5	NADH:ubiquinone oxidoreductase subunit B5
NDUFB10	NADH:ubiquinone oxidoreductase subunit B10
COX15	cytochrome c oxidase assembly homolog COX15
UQCRC1	ubiquinol-cytochrome c reductase core protein 1
HSDL2	hydroxysteroid dehydrogenase like 2
ALKBH3	alkB homolog 3, alpha-ketoglutaratedependent dioxygenase
FAHD1	fumarylacetoacetate hydrolase domain containing 1
ANXA6	annexin A6
SQSTM1	sequestosome 1

ATP5IF1	ATP synthase inhibitory factor subunit 1
ALAS1	5'-aminolevulinate synthase 1
LACTB	lactamase beta
HSCB	HscB mitochondrial iron-sulfur cluster cochaperone
PRKACA	protein kinase cAMP-activated catalytic subunit alpha
UBA1	ubiquitin like modifier activating enzyme 1
ABCB6	ATP binding cassette subfamily B member 6 (Langereis blood group)
MAP2K2	mitogen-activated protein kinase kinase 2
NAPG	NSF attachment protein gamma
RPS27A	ribosomal protein S27a
BCL2L11	BCL2 like 11
CAPN2	calpain 2
PNPLA7	patatin like phospholipase domain containing 7
FOXO3	forkhead box O3
NIPSNAP2	nipsnap homolog 2
VDAC3	voltage dependent anion channel 3
DNAJC11	DnaJ heat shock protein family (Hsp40) member C11
ACBD3	acyl-CoA binding domain containing 3
ABCB8	ATP binding cassette subfamily B member 8
GIMAP8	GTPase, IMAP family member 8
HCLS1	hematopoietic cell-specific Lyn substrate 1
PAM16	presequence translocase associated motor 16
PPP3CC	protein phosphatase 3 catalytic subunit gamma
MTCH2	mitochondrial carrier 2
DNAJC19	DnaJ heat shock protein family (Hsp40) member C19
PMPCA	peptidase, mitochondrial processing alpha subunit
PARL	presenilin associated rhomboid like
TIMM8B	translocase of inner mitochondrial membrane 8 homolog B
ACP6	acid phosphatase 6, lysophosphatidic
HDHD5	haloacid dehalogenase like hydrolase domain containing 5
GRAMD4	GRAM domain containing 4
FAM162A	family with sequence similarity 162 member A
URI1	URI1 prefoldin like chaperone
SLC25A24	solute carrier family 25 member 24
SLC25A20	solute carrier family 25 member 20
TFAM	"transcription factor A, mitochondrial
COA3	cytochrome c oxidase assembly factor 3
COX16	cytochrome c oxidase assembly factor COX16
FECH	ferrochelatase
TBRG4	transforming growth factor beta regulator 4
LACTB2	lactamase beta 2
POLDIP2	DNA polymerase delta interacting protein 2
DCAF8	DDB1 and CUL4 associated factor 8

SLC25A39	solute carrier family 25 member 39
CLIC4	chloride intracellular channel 4
SLC25A45	solute carrier family 25 member 45
SFXN2	sideroflexin 2
CHCHD5	coiled-coil-helix-coiled-coil-helix domain containing 5
KLC2	kinesin light chain 2
ARMC10	armadillo repeat containing 10
GLOD4	glyoxalase domain containing 4
CISD3	CDGSH iron sulfur domain 3
AKAP10	A-kinase anchoring protein 10
BOLA3	bolA family member 3
NIPSNAP3B	nipsnap homolog 3B

Supplementary references

[1] Heydtmann M, Hardie D, Shields PL, Faint J, Buckley CD, Campbell JJ, et al. Detailed analysis of intrahepatic CD8 T cells in the normal and hepatitis C-infected liver reveals differences in specific populations of memory cells with distinct homing phenotypes. J Immunol 2006;177:729-738.

[2] Wisniewski JR, Zougman A, Nagaraj N, Mann M. Universal sample preparation method for proteome analysis. Nat Methods 2009;6:359-362.

[3] Ficarro SB, Adelmant G, Tomar MN, Zhang Y, Cheng VJ, Marto JA. Magnetic bead processor for rapid evaluation and optimization of parameters for phosphopeptide enrichment. Anal Chem 2009;81:4566-4575.

[4] Wang Y, Yang F, Gritsenko MA, Wang Y, Clauss T, Liu T, et al. Reversed-phase chromatography with multiple fraction concatenation strategy for proteome profiling of human MCF10A cells. Proteomics 2011;11:2019-2026.

[5] Gilar M, Olivova P, Daly AE, Gebler JC. Two-dimensional separation of peptides using RP-RP-HPLC system with different pH in first and second separation dimensions. J Sep Sci 2005;28:1694-1703.

[6] Olsen JV, de Godoy LM, Li G, Macek B, Mortensen P, Pesch R, et al. Parts per million mass accuracy on an Orbitrap mass spectrometer via lock mass injection into a C-trap. Mol Cell Proteomics 2005;4:2010-2021.

[7] Ohradanova-Repic A, Machacek C, Charvet C, Lager F, Le Roux D, Platzer R, et al. Extracellular Purine Metabolism Is the Switchboard of

Immunosuppressive Macrophages and a Novel Target to Treat Diseases With Macrophage Imbalances. Front Immunol 2018;9:852.